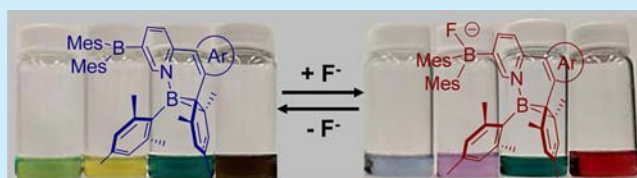


Tuning the Colors of the Dark Isomers of Photochromic Boron Compounds with Fluoride Ions: Four-State Color Switching

Soren K. Mellerup,[†] Ying-Li Rao,[†] Hazem Amarne,[§] and Suning Wang^{*,†,‡}[†]Department of Chemistry, Queen's University, Kingston, Ontario K7L 3N6, Canada[‡]Beijing Key Laboratory of Photoelectric/Electrophotonic Conversion Materials, School of Chemistry, Beijing Institute of Technology, Beijing 1000081, P. R. China[§]Department of Chemistry, The Hashemite University, P.O. Box 330117, Zarqa, 13133, Jordan

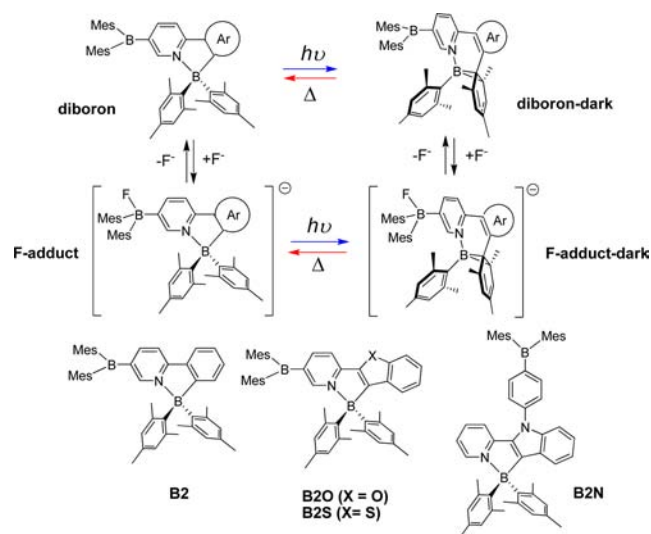
Supporting Information

ABSTRACT: Combining a three-coordinated boron (BMes₂) moiety with a four-coordinated photochromic organoboron unit leads to a series of new diboron compounds that undergo four-state reversible color switching in response to stimuli of light, heat, and fluoride ions. Thus, these hybrid diboron systems allow both convenient color tuning/switching of such photochromic systems, as well as visual fluoride sensing by color or fluorescent emission color change.



Molecular systems capable of undergoing discrete and readily reversible interconversion between various states are of great interest in materials science owing to their potential applicability in optical memory devices/switches¹ and molecular recognition.² Aside from well-known classes of chemical entities such as diarylethenes (DTEs)³ or spiropyran,⁴ boron-containing π -materials have begun to attract significant research attention within these fields as a result of their diverse reactivities and rich optoelectronic properties.⁵ We have recently demonstrated that four-coordinated N,C-organoboron chelates are capable of displaying efficient photochromic switching wherein a thermally reversible intramolecular C–C bond-forming/breaking reaction generates intensely colored B,N-embedded bisnorbornadienes with a general structure analogous to **diboron-dark** shown in Scheme 1.⁶ This reactivity stands in stark contrast to most other photochromic systems, which tend to undergo ring opening/closing processes upon exposure to light, and remains as one of only two⁷ examples of photochromic switching at a boron core. Nevertheless, organoboron subunits have found use as substituents in several DTE derivatives, wherein the boron fragments either allow the effective tuning of the DTE photochemical switching⁸ or display varying Lewis acidity in each available state.⁹ Based on these prior works and the propensity for triarylboron to bind with small anions such as fluoride,¹⁰ we postulated that substitution of our N,C-organoboron systems with BMes₂ could provide a simple and efficient strategy for modulating the colors of the dark isomers, achieving four-state switching as shown in Scheme 1. The dark isomers are in general stable toward water, which is often associated with fluoride ions, making it possible to use fluoride ions to tune/switch the colors of the photochromic boron-based systems. To demonstrate this, four diboron compounds—previously reported **B2** and three new molecules with different backbones (Scheme 1)—

Scheme 1. Four-State Switching and Structures of the Diboron Molecules



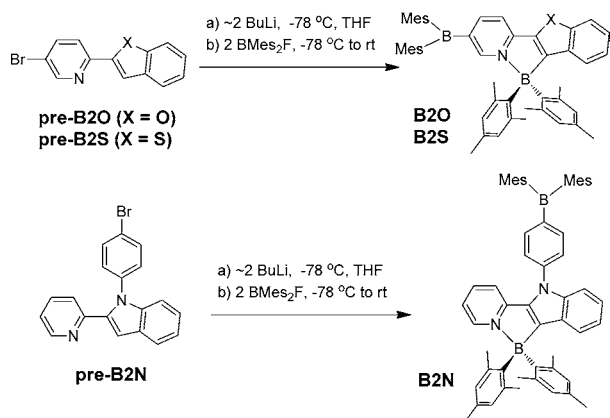
were prepared to establish the impact of the acceptor unit and its substitution position on the color switching of the boron system.

Compounds **B2O**, **B2S**, and **B2N** (**B2X**) were prepared in moderate yields via a one-step lithium–halogen exchange and deprotonation of the appropriate precursor (**pre-B2X**), followed by the addition of 2 equiv of FBMe₂, as shown in Scheme 2. **B2** was prepared as previously reported.^{6a} **B2X** compounds were fully characterized by ¹H, ¹³C, and ¹¹B NMR,

Received: August 3, 2016

Published: August 18, 2016

Scheme 2. Syntheses of the Diboron Compounds



HRMS, and elemental analysis (see Supporting Information, SI). The crystal structure of **B2O** was determined by single-crystal X-ray diffraction and is shown in Figure 1.

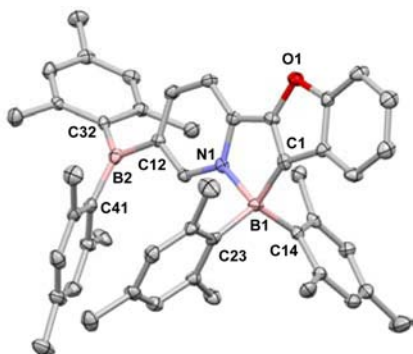


Figure 1. Crystal structure of **B2O**. H atoms were omitted for clarity. Key bond lengths (Å): B(1)–C(1) 1.631(7), B(1)–C(14) 1.628(7), B(1)–C(23) 1.641(8), B(1)–N(1) 1.668(6), B(2)–C(12) 1.574(7), B(2)–C(32) 1.566(8), B(2)–C(41) 1.554(8).

As shown in Figure 2 and summarized in Table 1, the diboron compounds all possess multiple intense absorption bands in the UV–vis spectra. Similar to previously reported N,C-organoboron chelates,⁶ all four molecules display a low energy band at ca. 410–430 nm. For **B2S** and **B2O**, the lower energy band is intense and well resolved while those of **B2** and **B2N** appear as shoulder peaks. From TD-DFT calculations, the primary contribution to the *S*₁ vertical excitation of **B2**, **B2O**, and **B2S** is HOMO (Mes of chelate boron; π) to LUMO (backbone plus the tricoordinated boron unit; π^*), which is assigned to their low energy absorption band. In contrast, for **B2N**, the *S*₁ state (422 nm band) is mainly from HOMO (Mes of chelate boron; π) to LUMO+1 (backbone, π^*) with little contributions from the triarylboron unit, while the *S*₂ is dominated by HOMO \rightarrow LUMO (BMes₂Ph, π^*) and responsible for the band at 376 nm. Consistent with this TD-DFT data, the addition of fluoride (tetrabutylammonium fluoride, TBAF) to **B2**, **B2O**, and **B2S** caused quenching of the low energy absorption band while, for **B2N**, it led to quenching of the band at 376 nm instead of the 410 nm shoulder band. Consequently, **B2N** experienced little color change after fluoride addition, while the other three diboron compounds all became colorless (Figure 2). The fluoride addition also caused a distinct change in their fluorescence

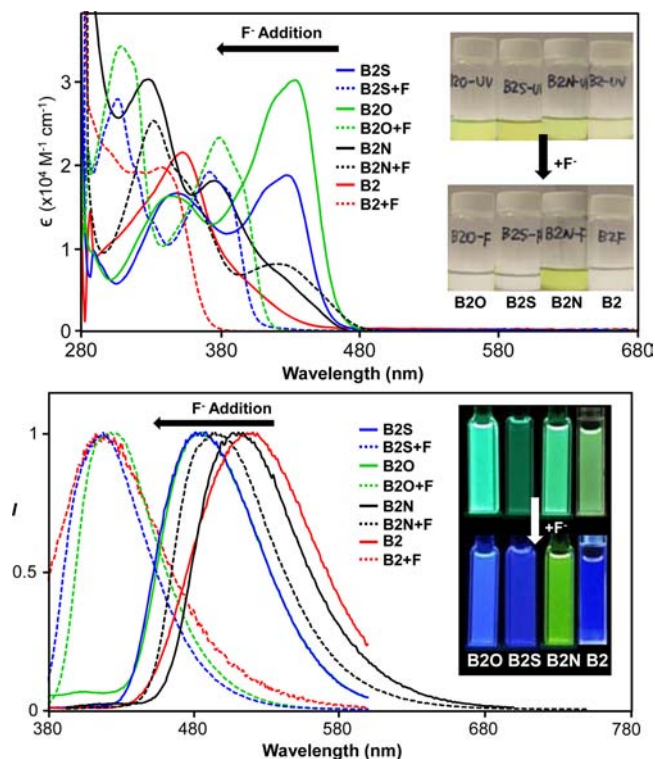


Figure 2. UV–vis (top) and fluorescence (normalized, bottom) spectra of **B2X** and **B2**, and their fluoride adducts in toluene at 10^{-5} M. Inset: Photographs showing the color and fluorescence color change before and after fluoride addition.

Table 1. Photophysical Properties of the Diboron Compounds

compd	λ_{abs} (nm) (ϵ , $\text{M}^{-1} \text{cm}^{-1}$) ^a	λ_{em} (nm) ^a	Φ^b
B2S	348, 426 (1.95×10^4)	488	0.18
B2O	345, 434 (3.14×10^4)	489	0.79
B2N	328, 376, 422 (0.691×10^4)	495	0.56
B2	352, 410 (0.443×10^4)	525	0.33

^a 1.0×10^{-5} M in toluene at 298 K. ^bQY in solution, determined relative to quinine hemisulfate.¹¹

spectra. For **B2**, **B2O**, and **B2S** the fluorescence spectra experienced a hypsochromic shift with fluoride addition, to $\lambda_{\text{em}} = \sim 420$ nm and emission color change from blue-green/green to blue. For **B2N**, its fluorescence spectrum displayed a small hypsochromic shift of ~ 15 nm and the emission color changed from blue-green to green (Figure 2, bottom). In all cases, the *F*[−] binding constants were determined to fall within $(2.1\text{--}2.7) \times 10^4$ (± 0.5) M^{-1} , which are consistent with previous reported values of triarylboron compounds.¹⁰

All three **B2X** compounds undergo photoisomerization in the same manner as **B2** upon UV irradiation at 350 nm yielding their respective dark isomers **B2O-dark**, **B2S-dark**, and **B2N-dark**, as evidenced by UV–vis spectroscopy (Figure 3 and SI) which shows the appearance of new low-lying absorption bands between 650 and 750 nm and distinct colors (green, **B2O**; yellow, **B2S**; turquoise, **B2N**; brown, **B2**). In accordance with previous findings,⁶ TD-DFT calculations suggest that all four bands of the diboron dark isomers originate from HOMO (π) to LUMO (π^* -backbone-BMes₂) CT transitions, with the HOMO located on the boracycle and the cyclohexadienyl ring (see SI). Due to the similar HOMO orbitals of all four dark

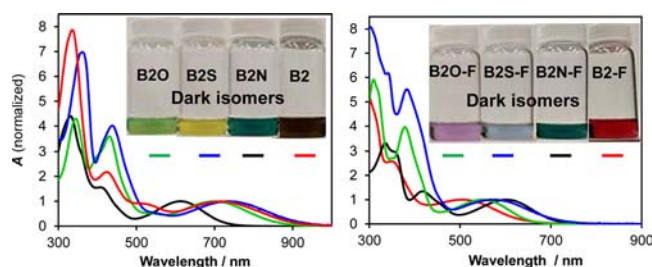


Figure 3. UV-vis spectra of the **B2X** and **B2** dark isomers (left) and **B2X-F** and **B2-F** dark isomers (right) in toluene at 10^{-4} M. Inset: Photographs showing the colors of the dark isomers.

isomers, their unique solution colors are caused by the variations in their LUMO energy levels, which are governed by the π^* orbitals of the chelating ligands. The ^1H and ^{11}B NMR spectra showed that all diboron compounds undergo clean and quantitative transformation to the dark isomers (see SI) with photoisomerization quantum efficiencies (Φ_{PI}) similar to their monoboron counterparts^{6a,d} (<0.10 for **B2X** and 0.83 for **B2**). The low Φ_{PI} of **B2X** compounds is in agreement with the previous findings, which showed that extending the π -backbone of the chelating ligand results in stabilization of the excited state, hence decreasing their photoreactivity.^{6b} All diboron dark isomers readily undergo thermal conversion back to their original light colored state when heated at 70°C (several hours at typical NMR concentrations).

Next we examined the photoswitching of the fluoride adducts of **B2X** and **B2** in solution. All four fluoride adducts undergo photoisomerization in the same manner as the nonfluoride bound parent molecules, as confirmed by UV-vis and NMR spectroscopy (see SI). Most interesting is that the colors of the dark isomers of the fluoride adducts are distinctly different from those of the parent molecule with the exception of **B2N-F-dark** and **B2N-dark** which have a similar turquoise color (Figure 3). As shown in Figure 3 and Table 2, F-bound dark isomers of the three compounds with BMes_2 substituted on the pyridine ring display a dramatic hypsochromic shift in their low energy absorption λ_{max} compared to the non-F bound dark isomers. This is rationalized whereby the formation of the fluoride adducts results in destabilization of the LUMO energy level, creating larger optical gaps (E_g) which manifest themselves as higher absorption energies. Conversely, the absorption band of **B2N-F-dark** shows only a 10 nm bathochromic shift of its absorption band compared to **B2N-dark**. In fact, the colors of **B2N-F-dark** and **B2N-dark** are similar to the related monoboron compound, lacking the three-coordinated BMes_2 .^{6c} This difference can be explained by the contributions of the BMes_2 unit to the LUMO level. For **B2O-dark**, **B2S-dark**, and **B2-dark**, the p_π orbital of the B atom dominates the π^* (LUMO) orbital, while its contribution to the LUMO is far less pronounced in **B2N-dark** with the phenyl linker of the BMes_2 unit lying almost perpendicular to the indolyl ring (see

SI). As a result, the fluoride ion has a minimal impact on the color of **B2N-dark**. This supports that direct attachment of a BMes_2 unit at the 5-position on the pyridyl ring is an effective approach in achieving color tuning of the dark isomers using fluoride ions. **B2X-F-dark** and **B2-F-dark** can be readily converted to **B2X-dark** and **B2-dark** by simply washing the toluene/benzene solution of the F-bound dark isomers with water, which removes the fluoride ion (see SI). Furthermore, as in the case of the non-F bound dark isomers, the F-dark isomers can thermally revert back to the colorless isomers upon heating.

It is worth noting that completely photoconverting the diboron compounds to their dark isomers first and subsequently adding TBAF generates the same F-bound dark isomers **B2-F-dark**/**B2X-F-dark** as those obtained from the direct photoisomerization of the F-bound diboron compounds **B2** and **B2X** (see SI). Thus, reversible four-state switching can be achieved for these diboron compounds. This unusual multistate color switching facilitated by light, heat, and fluoride ions is illustrated in Figure 4 using **B2** as an example. All

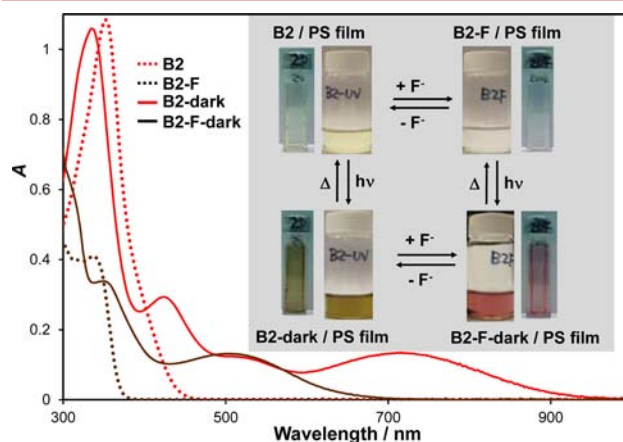


Figure 4. Four-state reversible switching of **B2**: UV-vis spectra of the four diboron species involved in the four-state color switching of **B2**. Inset: A diagram showing the distinct colors of the four states based on **B2** in polystyrene (PS) films (coated on the inside of a cuvette) and in toluene (vials).

diboron compounds and their F-bound adducts also undergo photoisomerization when doped in polystyrene matrices, generating the same dark isomers as in solution (Figure 4 and SI).

To demonstrate the stability of the diboron systems toward repeated photo- and thermal switching, **B2**, **B2-F**, **B2N**, and **B2N-F** were cycled through their photochromic states several times as representative examples for this class of molecules. As shown in Figure 5, both **B2** and **B2-F** compounds are capable of undergoing several rounds of photo- and thermal switching with the **B2-F** derivative exhibiting worse fatigue following

Table 2. Photophysical Properties of the Dark Isomers

compd	λ_{abs} (nm) ^a	color	compd	λ_{abs} (nm) ^a	color
B2S-dark	736	yellow	B2S-F-dark	575	blue-gray
B2O-dark	704	yellow-green	B2O-F-dark	548	purple
B2N-dark	614	turquoise	B2N-F-dark	604	turquoise
B2-dark	715	brown	B2-F-dark	502	red

^aAll data acquired in toluene at 10^{-4} M.

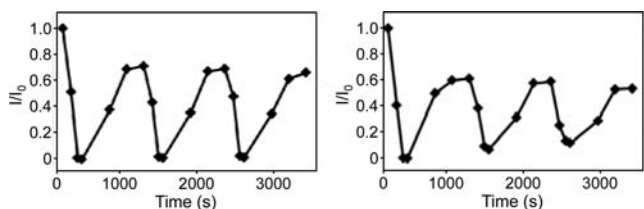


Figure 5. Diagrams showing the conversion of **B2** → **B2-dark** → **B2** (left) and **B2-F** → **B2-F-dark** → **B2-F** (right) over three cycles of irradiation (300 nm) and heating (90 °C) in C_6H_6 . I/I_0 is the ratio of fluorescence intensity at t vs fluorescence intensity at t_0 .

three repeated cycles. This may be attributed to the presence of trace oxygen entered the system as a result of the long heating time required for thermal reversal (~ 20 min at 10^{-5} M). Both **B2N** and **B2N-F** were found to undergo comparable performance in their cycling experiments (see SI), with the fluoride adduct once again showing more fatigue after the repeated cycling.

In conclusion, three new BMe_2 appended N,C-chelate organoboron compounds have been prepared and studied. The diboron compounds undergo photochromic switching in both solution and polymer films yielding their dark isomer states with varying color depending on the respective LUMO energy level. The addition of fluoride causes a distinct color change of **B2S**, **B2O**, and **B2** dark isomers. Due to distal BMe_2 substitution and poor conjugation with the chelate backbone in **B2N**, the dark isomers of **B2N** and **B2N-F** have similar colors and absorption spectra, indicating that the position of the pendent boron unit is critical for effective color modulation using fluoride ions. Four-state color switching with light, heat, and fluoride ions as the external stimuli has been established for the diboron compounds.

■ ASSOCIATED CONTENT

Supporting Information

The Supporting Information is available free of charge on the ACS Publications website at DOI: 10.1021/acs.orglett.6b02308.

Figures and tables of all characterization data, TD-DFT calculation data, additional UV-vis and fluorescence data of **B2** and **B2X**, their dark isomers, and X-ray data for **B2O** (PDF)

■ AUTHOR INFORMATION

Corresponding Author

*E-mail: wangs@chem.queensu.ca.

Notes

The authors declare no competing financial interest.

■ ACKNOWLEDGMENTS

The authors thank the Natural Science and Engineering Research Council (NSERC, RGPIN1193993-2013) of Canada for financial support. S.K.M. and Y.L.R. thank the Canadian Government for their Vanier Scholarships.

■ REFERENCES

(1) (a) Irie, M. *Chem. Rev.* **2000**, *100*, 1685–1716. (b) Irie, M.; Fukaminato, T.; Matsuda, K.; Kobatake, S. *Chem. Rev.* **2014**, *114*, 12174–12277. (c) Feringa, B. L.; van Delden, R. A.; Koumura, N.; Geertsema, E. M. *Chem. Rev.* **2000**, *100*, 1789–1816. (d) Yamashita,

H.; Ikezawa, T.; Kobayashi, Y.; Abe, J. *J. Am. Chem. Soc.* **2015**, *137*, 4952–4955. (e) Jia, C.; Migliore, A.; Xin, N.; Huang, S.; Wang, J.; Yang, Q.; Wang, S.; Chen, H.; Wang, D.; Feng, B.; Liu, Z.; Zhang, G.; Qu, D.-H.; Tian, H.; Ratner, M. A.; Xu, H. Q.; Nitzan, A.; Guo, X. *Science* **2016**, *352*, 1443–1445. (f) Zhang, J. L.; Zhong, J. Q.; Lin, J. D.; Hu, W. P.; Wu, K.; Xu, G. Q.; Wee, A. T. S.; Chen, W. *Chem. Soc. Rev.* **2015**, *44*, 2998–3022.

(2) (a) Nolan, E. M.; Lippard, S. J. *Acc. Chem. Res.* **2009**, *42*, 193–203. (b) Nolan, E. M.; Lippard, S. J. *J. Am. Chem. Soc.* **2003**, *125*, 14270–14271. (c) Coskun, A.; Akkaya, E. U. *J. Am. Chem. Soc.* **2005**, *127*, 10464–10465. (d) Valeur, B.; Leray, I. *Coord. Chem. Rev.* **2000**, *205*, 3–40. (e) Hirai, M.; Gabbai, F. P. *Angew. Chem., Int. Ed.* **2015**, *54*, 1205–1209. (f) Christianson, A. M.; Gabbai, F. P. *Inorg. Chem.* **2016**, *55*, 5828–5835. (g) Choi, B. H.; Lee, J. H.; Hwang, H.; Lee, K. M.; Park, M. H. *Organometallics* **2016**, *35*, 1771–1777.

(3) (a) Tian, H.; Yang, S. *Chem. Soc. Rev.* **2004**, *33*, 85–97. (b) Raymo, F. M. *Phys. Chem. Chem. Phys.* **2013**, *15*, 14840–14850. (c) Irie, M.; Uchida, K. *Bull. Chem. Soc. Jpn.* **1998**, *71*, 985–996. (d) Irie, M.; Morimoto, M. *Pure Appl. Chem.* **2009**, *81*, 1655–1665. (e) Szalóki, G.; Pozzo, J.-L. *Chem. - Eur. J.* **2013**, *19*, 11124–11132.

(4) (a) Berkovic, G.; Krongauz, V.; Weiss, V. *Chem. Rev.* **2000**, *100*, 1741–1754 and references therein. (b) Day, J. H. *Chem. Rev.* **1963**, *63*, 65–80. (c) Lukyanov, B. S.; Lukyanova, M. B. *Chem. Heterocycl. Compd.* **2005**, *41*, 281–311. (d) Klajn, R. *Chem. Soc. Rev.* **2014**, *43*, 148–184. (e) Minkin, V. I. *Chem. Rev.* **2004**, *104*, 2751–2776.

(5) (a) Bagutski, V.; Grosso, A. D.; Carrillo, J. A.; Cade, I. A.; Helm, M. D.; Lawson, J. R.; Singleton, P. J.; Soloman, S. A.; Marcelli, T.; Ingleson, M. J. *J. Am. Chem. Soc.* **2013**, *135*, 474–487. (b) Loudet, A.; Burgess, K. *Chem. Rev.* **2007**, *107*, 4891–4932. (c) Li, D.; Zhang, H.; Wang, Y. *Chem. Soc. Rev.* **2013**, *42*, 8416–8433. (d) Entwistle, C. D.; Marder, T. B. *Angew. Chem., Int. Ed.* **2002**, *41*, 2927–2931. (e) Poon, C.-T.; Wu, D.; Yam, V. W. -W. *Angew. Chem., Int. Ed.* **2016**, *55*, 3647–3651.

(6) (a) Rao, Y.-L.; Amarne, H.; Zhao, S.-B.; McCormick, T. M.; Martić, S.; Sun, Y.; Wang, R.-Y.; Wang, S. *J. Am. Chem. Soc.* **2008**, *130*, 12898–12900. (b) Amarne, H.; Baik, C.; Murphy, S. K.; Wang, S. *Chem. - Eur. J.* **2010**, *16*, 4750–47610. (c) Amarne, H.; Baik, C.; Wang, R.-Y.; Wang, S. *Organometallics* **2011**, *30*, 665–668. (d) Rao, Y.-L.; Wang, S. *Inorg. Chem.* **2011**, *50*, 12263–12274. (e) Rao, Y.-L.; Amarne, H.; Wang, S. *Coord. Chem. Rev.* **2012**, *256*, 759–770. (f) Rao, Y.-L.; Chen, L. D.; Mosey, N. J.; Wang, S. *J. Am. Chem. Soc.* **2012**, *134*, 11026–11034. (g) Rao, Y.-L.; Amarne, H.; Chen, L. D.; Brown, M. L.; Mosey, N. J.; Wang, S. *J. Am. Chem. Soc.* **2013**, *135*, 3407–3410. (h) Rao, Y.-L.; Hörl, C.; Braunschweig, H.; Wang, S. *Angew. Chem., Int. Ed.* **2014**, *53*, 9086–9089.

(7) For examples of the other refer to: (a) Kano, N.; Yoshino, J.; Kawashima, T. *Org. Lett.* **2005**, *7*, 3909–3911. (b) Yoshino, J.; Kano, N.; Kawashima, T. *Tetrahedron* **2008**, *64*, 7774–7781.

(8) (a) Poon, C.-T.; Lam, W. H.; Wong, H.-L.; Yam, V. W. -W. *J. Am. Chem. Soc.* **2010**, *132*, 13992–13993. (b) Yang, Y.; Hughes, R. P.; Aprahamian, I. *J. Am. Chem. Soc.* **2012**, *134*, 15221–15224. (c) Ma, J.; Cui, X.; Wang, F.; Wu, X.; Zhao, J.; Li, X. *J. Org. Chem.* **2014**, *79*, 10855–10866. (d) Yang, Y.; Hughes, R. P.; Aprahamian, I. *J. Am. Chem. Soc.* **2014**, *136*, 13190–13193.

(9) (a) Zhou, Z.; Xiao, S.; Xu, J.; Liu, Z.; Shi, M.; Li, F.; Yi, T.; Huang, C. *Org. Lett.* **2006**, *8*, 3911–3914. (b) Lemieux, V.; Spantulescu, M. D.; Baldrige, K. K.; Branda, N. R. *Angew. Chem., Int. Ed.* **2008**, *47*, 5034–5037. (c) Poon, C.-T.; Lam, W. H.; Yam, V. W. -W. *J. Am. Chem. Soc.* **2011**, *133*, 19622–19625.

(10) (a) Yamaguchi, S.; Akiyama, S.; Tamao, K. *J. Am. Chem. Soc.* **2001**, *123*, 11372–11375. For select reviews on the topic, see: (b) Wade, C. R.; Broomsgrange, A. E. J.; Aldridge, S.; Gabbai, F. P. *Chem. Rev.* **2010**, *110*, 3958–3984. (c) Hudnall, T. W.; Chiu, C.-W.; Gabbai, F. P. *Acc. Chem. Res.* **2009**, *42*, 388–397. (d) Galbraith, E.; James, T. D. *Chem. Soc. Rev.* **2010**, *39*, 3831–3842. (e) Zhao, H.; Leamer, L. A.; Gabbai, F. P. *Dalton Trans.* **2013**, *42*, 8164–8178.

(11) Brouwer, A. M. *Pure Appl. Chem.* **2011**, *83*, 2213–2228.